

Functional Mode Switching for Safe and Efficient Human-Robot Interaction

Petr Svarny*, Mazin Hamad*, Alexander Kurdas,
Matej Hoffmann, Saeed Abdolshah, and Sami Haddadin

Abstract— Various approaches can ascertain the safety and efficiency of physical human-robot collaboration. This paper presents the concept of robot functional mode switching to efficiently ensure human safety during collaborative tasks based on biomechanical pain and injury data and task information. Besides the robot's reflected inertial properties summarizing its impact dynamics, our concept also integrates safe and smooth velocity shaping that respects human partner motion, interaction type, and task knowledge. We further discuss different approaches to safely shape the robot velocity without sacrificing the overall task execution time and motion smoothness. The experimental results showed that our proposed approaches could decrease jerk level during functional mode switching and limit the impact of safety measures on productivity, especially when guided with additional task knowledge.

I. INTRODUCTION

In the industrial context, safety in physical human-robot interaction (pHRI) scenarios is a highly discussed and investigated topic. However, it can be surrounded by some controversy due to the requirements imposed on collaborative robots by the ISO/TS 15066:2016 [1] specification that are perceived as overly conservative (for example, see discussion in [2] or [3]). Part of the discussion is that the limit for safe interaction is given not by injury but by the onset of pain; nevertheless, in the context of non-industrial¹ (e.g., service) robots, these strict requirements seem well-placed (hinted already in [5]).

The safety of non-industrial robots is usually satisfied by the use of lightweight design and covered by other standards, e.g., ISO 13482 [5] [6]. However, we can also apply lessons from collaborative industrial robots to improve robot control in pHRI scenarios with non-industrial robots. An industry-inspired collaboration scenario is demonstrated on a Franka Panda arm as shown in Fig. 1, where the human partner safety has to be always ensured. The results can, however, be extended also to a humanoid GARMi robot [7] that is equipped with two Franka Panda robot arms². In this work, we envision a situation where a humanoid robot would collaborate with the user on a task with close pHRI. We apply the industrial experience to this non-industrial context.

The remainder of this article is organized as follows. Section II summarizes the theoretical background, followed by our methodology in Section III. Thereafter, the experimental work utilizing the proposed functional mode

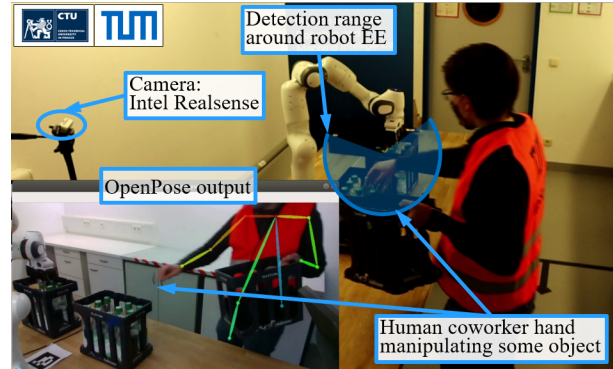


Fig. 1: Experiment setup and OpenPose [9] view visualization.

switching approach is presented in Section IV. The results are discussed in Section V. Section VI concludes the paper and highlights future research directions.

II. BACKGROUND & PRELIMINARIES

Vicentini [10] pointed out that the terminology used for task definition in the industry is ill-suited for determining the technical aspects related to the robotic application's safety. Therefore, the investigation of a pHRI scenario can be viewed from two perspectives: interaction and safety. As these perspectives cannot be matched as a simple one-to-one correspondence, we treat them separately first then combine them into so-called functional modes. Even though these perspectives originate in industrial settings, robotic systems in non-industrial contexts can still benefit from them.

Another aspect we address in this manuscript is the smooth transition between various robot modes because this facilitates implementing efficient human-robot interaction (see Sec. II-B).

A. Perspectives on physical human-robot interaction

The two perspectives address different goals. Interaction modes describe what should be the nature of the pHRI, and safety regimes describe how the safety during these interactions is ascertained.

1) *Interaction modes*: We can distinguish four interaction modes. As Vicentini [10] argues, the terminology connected to interaction is used inconsistently, and various sources can intend different behavior while referring to the same interaction mode. However, we could generally present the interaction modes as a hierarchy. Based on the early works [11], [12], these would be from the least interactive to the most interactive:

Autonomous mode: there is no shared workspace and no shared task purpose.

Coexistence: the human and the robot share the workspace but do not have a shared task purpose.

Cooperation: coexistence with a shared task purpose.

*Shared first authorship; the two authors contributed equally.

Petr Svarny and Matej Hoffmann are with the Department of Cybernetics, Faculty of Electrical Engineering, Czech Technical University in Prague. Mazin Hamad, Alexander Kurdas, Saeed Abdolshah, and Sami Haddadin are with the Chair of Robotics and Systems Intelligence, Munich Institute of Robotics and Machine Intelligence, Department of Computer Engineering, School of Computation, Information and Technology, Technische Universität München (TUM).

svarnpet@fel.cvut.cz, mazin.hamad@tum.de

¹We use the general term "non-industrial (humanoid) robot" deliberately as the delimitation given in the standards can be problematic (see [4]).

²See additional examples in the concept video [8].

Collaboration: cooperation that allows contact between the human partner and the robot.

These interaction modes can be incorporated explicitly, i.e., made part of the robot's controller, for example, in the form of a finite-state safety automaton as proposed by Haddadin et al. [13]. One last mode worth mentioning, even though it stands on the side of this hierarchy, is the fault reaction mode. This mode does not presume any interaction between the human and the robot as it expects the robot to stay still while the human clears any cause of the fault. In our context, four modes will be used, as visible in Fig. 3.

2) *Safety regimes*: Safety of pHRI has been discussed extensively in various surveys (see [14], [15], or with the focus on collaboration [16]). Various standards are often used to determine if the robotic application is safe. Especially it is the ISO/TS 15066 [1] in the industrial context that addresses the safety of collaborative robots. The standard defines four safety regimes for collaborative operation. Therefore, as opposed to the interaction modes, these four regimes are clearly defined and can be summed up as:

Safety-rated Monitored Stop (SMS): the robot stops as soon as the human enters the defined workspace.

Hand-Guiding (HG): the human uses a guiding device near or at the end-effector to transmit motion commands to the robot.

Speed and Separation Monitoring (SSM): a collision avoidance method by monitoring the positions and velocities of both the human partner and the robot.

Power and Force Limiting (PFL): the robot is designed or controlled so that any potential collision does not exceed the allowed collision force limits (i.e., safety thresholds).

The choice of safety regime leads to various challenges (e.g., proper tracking of the human partner in SSM). These challenges are addressed in relevant research (for an example of a vision-based safety approach, see [17]). In a non-industrial context, it is often a PFL-like approach that is being applied or SMS. For example, see the sociable humanoid robot *Pepper* with its safe motor performance [18], which still can present risks in pHRI [19].

We investigate a close collaboration task between humans and robots that can lead to potentially dangerous situations. Such situations can be solved in multiple ways. Prominent examples close to our approach are found in [20], where human motion tracking is integrated with optimization techniques, and in [21], where human tracking is used for fast trajectory replanning. The most formidable example of such research is the progression of the work of Zanchettin et al. [22]–[25]. The initial paper [22] implemented functional modes similar to those of the coworker automaton from [13] and implemented a collaboration operation meeting the demands of SSM. The following papers improve on the SSM-compliant collaboration by predicting the partner's movements [23] or calculating the optimal avoidance path [24]. Finally, the authors also implemented a combination of SSM and PFL safety regimes in [25].

B. Smooth interaction

Scenarios of direct pHRI, namely hand-over tasks as presented in [26], suggest that smooth, minimal-jerk movements on the robot side improve the task execution by the human partner. For industrial context, the effect of unexpected robot movements on the human was investigated

in [27] and led to the suggestion of a specific unit that could account for the human perception of psychological safety [28]. Therefore, any changes between robot functional modes and applied velocities should be smooth to make the interaction not only efficient but also pleasant.

Contributions

Our core contribution is incorporating the intended interaction modes as input parameters of the robot control in addition to the usual inputs, e.g., human detection, distance, velocity. The integration of the intended interaction mode then allows us to modulate how safety is ascertained, i.e., SSM/PFL modes and transition between them. We call this approach Functional Mode Switching (FMS). Our contributions can be summarized as follows:

- 1) Human-robot interaction modes (collaboration, cooperation, coexistence, autonomous behavior) as input parameters that modulate the behavior of the robot automaton and the use of industrial safety regimes (SSM and PFL).
- 2) Smooth velocity shaping method that allows switching between various safety regimes and evaluation of this shaping under various criteria.
- 3) Transfer of industrial safety experience to non-industrial settings.

III. METHODOLOGY

A. Human pose and velocity estimation

For estimating the position and velocity of different human keypoints, we rely on the setup for keypoint-wise distance measurement in [29]. The human keypoints are obtained from a vision processing pipeline that uses an RGB-D camera (Intel RealSense D435) to capture the image and OpenPose [9] with the BODY 25 model for the identification of human keypoints. Image processing is done with OpenCV3 [30] running on a PC with a dedicated GPU. The 3D velocity vector of the human keypoints was calculated from the 3D position change with simple differentiation and a moving average filter over a short past horizon to avoid jumps. See the setup in Fig. 1.

B. Relative velocity calculation

We use the Safe Motion Unit (SMU) framework [2] that calculates a biomechanically safe task velocity v^{SMU} based on the relative human-robot velocity and the appropriate force limits. Three collision-relevant situations can be distinguished based on the robot and human motions:

- (i) both partners are moving towards each other,
- (ii) both are moving in the same direction with the robot being behind the human and moving faster,
- (iii) the opposite case: the human follows the robot.

The effective speed of an impact v_{impact} is the highest in case (i). To mitigate the human injury risk, it must hold for the point of interest (POI), in our case end-effector (EE), velocity v_{EE} and human velocity v_H that³:

$$v_{\text{impact}} = \|v_{\text{EE}} - v_H\| \leq v^{\text{SMU}}. \quad (1)$$

Regarding case (ii), the robot can be allowed to move with a velocity faster than v^{SMU} according to Eq. 1. However, if

³We use superscripts for commanded values and subscripts for observed values, e.g., v^{SMU} is commanded. In contrast, v_{EE} is observed.

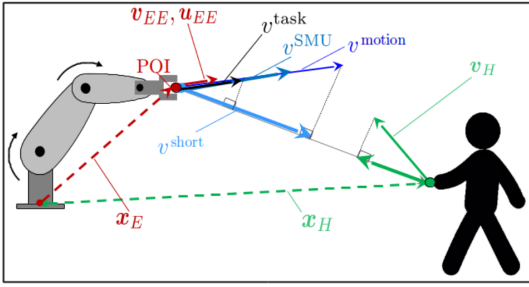


Fig. 2: An exemplary interaction case in which the robot end-effector is moving in the direction \mathbf{u}_{EE} . Presented are the required position and velocity vectors for both the human ($\mathbf{x}_H, \mathbf{v}_H$) and robot ($\mathbf{x}_{EE}, \mathbf{v}_{EE}$) as also the projections onto the line connecting the human and end-effector locations, the desired task speed v^{task} , and safe velocity limit v^{SMU} .

the human suddenly stops, the collision would be unsafe. Hence, v^{SMU} is used as the task safety threshold.

In case (iii), v_{EE} can be set equal to v^{task} , i.e., the velocity defined by the task. Velocity shaping cannot prevent collisions in this case as the robot would have to possibly exceed its desired value v^{task} to prevent a collision. Since the robot task velocity is commanded based on the relative velocity to the human, one may think it would be better to command a higher task velocity in case the human velocity exceeds v^{SMU} to escape collision. However, this would lead to a possibly unsafe robot velocity as in case (i). To assure a deterministic behavior of the robot in such cases, a practical solution is to set a lower limit for the task velocity resulting in a robot speed close to a standstill; we used $v^{low} = 0.1$ m/s.

We compared the following three shaping approaches with the baseline without human presence (v^{task} in our experimental validation).

- v^{motion} : relative velocity as projected velocity in the direction of the POI's motion,
- v^{short} : relative velocity as projected in the direction of the shortest distance between the human and the POI,
- v^{SMU} : uses only a distance threshold and shapes velocity based on the SMU's commanded velocity.

The difference between these shaping approaches lies in the way the relative velocity between the human and robot is being treated. Two approaches are given by the calculation of the relative projected velocity of the POI, i.e., point on the robot considered for the expected collision incident. In both these two cases, one does not use any projection. Moreover, the POIs can be chosen freely and could even encompass the whole body of the robot. The choice of a specific POI, however, does not change the principle of the presented approach as it can be recursively applied to all chosen POIs. Then the POI resulting in the most conservative robot velocity is to be adopted. For our study, we chose only the robot end-effector, EE, as a single POI.

A unit vector \mathbf{u}_c is determined based on the chosen projection, either for v^{motion} or v^{short} . We calculate the projection of \mathbf{v}_{EE} onto the chosen unit vector \mathbf{u}_c as:

$$\text{proj}_{\mathbf{u}_c} \mathbf{v}_{EE} = \left(\frac{\mathbf{v}_{EE} \cdot \mathbf{u}_c}{|\mathbf{u}_c|} \right) \frac{\mathbf{u}_c}{|\mathbf{u}_c|} \quad (2)$$

Therefore, for a chosen projection and thus velocity of choice v^c , the Eq. 1 must hold, i.e.:

$$v^c = \|\text{proj}_{\mathbf{u}_c} \mathbf{v}_{EE} - \text{proj}_{\mathbf{u}_c} \mathbf{v}_h\| \leq v^{SMU}. \quad (3)$$

C. Robot functional modes

In the following, we present our approach for safely and efficiently executing collaborative tasks. Given the biomechanical safety limits and task knowledge, our approach avoids stopping the interaction (except for faults). Instead, the desired task velocity is only reduced as needed. In our work, we primarily use distance thresholds for switching between the functional modes. We use the relative distance d_{rel} that is measured between the human keypoint (e.g., the wrist \mathbf{x}_{wrist}) and a chosen robot POI (EE in our case), i.e., $d_{rel} = |(\|\mathbf{x}_{EE}\| - \|\mathbf{x}_H\|)|$, see Fig. 2. However, more complex switching behavior could be implemented (e.g., based on the task's state).

Additionally, we introduce the *safe performance index SP*, i.e., the fraction of the velocity that should be used. The value of *SP* can be continuously updated online to reflect the desired safety level of the task execution. Its value can be derived from, e.g., percentage of braking distance of the robot, task and interaction knowledge, user studies, etc. This index gives the human some control over the robot's functional mode switching and task execution. For example, it can be set to force the robot to continue in the current mode or to switch into another mode by disregarding or overriding the automaton logical state transition functions based on task-relevant knowledge or partner experience. Adding this feature provides high flexibility for collaborative task execution under safety and performance considerations. Therefore, functional modes are switched based on the task specification or the current minimum distance between the observed points (unless there is a fault signal).

The collaborative task productivity may be lowered efficiently by switching to a safe robot operational mode only when necessary. By visually tracking the location of the human partner, flexible, near-real-time state transitions (below 1 ms) are ensured. For this, the robot dynamically switches between pre-specified functional modes that combine the interaction modes and safety regimes to increase the effectiveness of the interaction between the robot and the human partner. To provide a sufficient number of options for generic operational cases relevant to collaborative workspaces, we distinguish between four functional modes of the robot in pHRI scenarios (see Fig. 3):

- 1) Autonomous mode (*AM*),
- 2) Fault reaction mode (*FR*),
- 3) Coexistence mode (*Coex*),
- 4) Collaborative mode (*Col*),

Note that the *cooperative mode* from Sec. II-A.1 was omitted as it is not used during our example task.

Autonomous mode

In the autonomous mode, the task can be executed safely and autonomously while the human is outside the robot's workspace. The robot carries out the task under specific optimality criteria, such as cycle time, leading to the full desired task speed to maximize productivity.

Fault reaction mode

The robot reaches a fault state. Therefore the robot motion is stopped until the fault is checked and cleared by the human partner and the task execution can be recovered again.

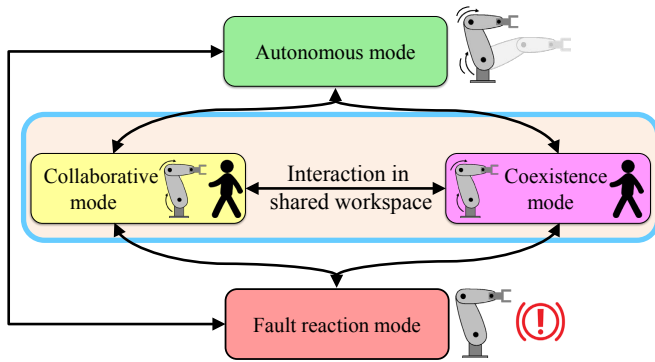


Fig. 3: The robotic coworker automaton, based on [13].

Coexistence mode

In this mode, the human and the robot share a common physical coexistence workspace, i.e., the relative distance between the robot and human is lower than a predefined coexistence threshold, $d_{\text{rel}} < d^{\text{coex}}$. Therefore, the desired task speed is lowered to ensure safety. The workspace is defined dynamically around the robot POI. However, no direct contact or interaction between the human and the robot is expected and therefore safety is provided by a combination of SSM and PFL. This is achieved by reducing the task velocity to respect the biomechanical safe limit v^{SMU} by optimal braking strategies, but only in cases where a collision is expected (see situations in Sec. III-B).

Collaboration mode

Contrary to the no-interaction assumption for coexistence, collaborative tasks mostly involve closer physical interactions between the robot and human, i.e., $d_{\text{rel}} \leq d^{\text{col}} < d^{\text{coex}}$. The assumption of frequent human-robot contacts puts more focus on lowering the velocity, i.e., PFL regime, so that the relative velocity of a physical collision does not exceed v^{SMU} . The collaboration mode's triggering also depends on the current interaction scenario (see Sec. III-B).

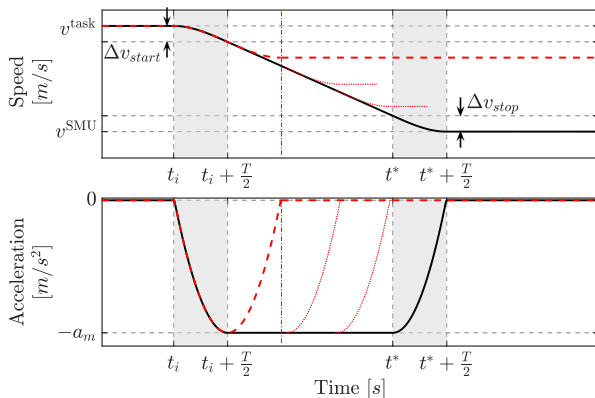


Fig. 4: The basic idea of a general solution for the adaptive shaping of the robot speed using linear velocity blends. The dotted red lines indicate arbitrary possible target speeds v_d^* , at which the shaping algorithm might leave the linear part. The values Δv_{start} and Δv_{stop} indicate the minimum change of speeds that can be carried out by the robot due to its acceleration. The times t_i, t^* indicate the onset of the acceleration and braking, respectively. Following these, the bold dashed line indicates the minimum increment in speed change given by the acceleration behavior.

D. Smooth velocity shaping

We investigate velocity shaping, a necessity for coexistence and collaboration modes. There are several ways to adapt

the speed v with which a robot executes a preplanned motion profile while preserving both a safe and smooth trajectory. Based on task knowledge, key trajectory points of the underlying interpolator, and desired smoothness of the resulting motion, polynomial functions with higher degrees than the number of conditions to be satisfied can be used. For example, a fifth-order polynomial allows adapting the robot trajectory to arbitrary values with boundary conditions also in acceleration [31].

Assume that there are two given levels of speed between which the robot motion has to be adapted starting at time instant t_i (see also Fig. 4). The robot must transition from current speed v_i at position s_i to desired speed v_d at position s_d without violating the constraint on maximum acceleration a_m . To avoid jerky motions during velocity shaping, position, speed, and acceleration profiles along the direction of motion must be smooth. The shaping consists of three phases: raising the acceleration to its maximum value a_m , constant acceleration, and acceleration reduction to zero. Only the first phase is completely precalculated. The length of the other two phases is determined based on the current desired velocity v_d^* – see dotted lines in Fig. 4.

IV. EXPERIMENTS

For validation, we set up two main experiments. The “Comparison experiment” involves executing two tasks with different intended interaction modes. The goal is to compare the performance of various velocity-shaping approaches under different robot functional modes. The “Grasping experiment” demonstrates the safe execution of a generic collaborative grasping task using our proposed robot *Functional Modes Switching* concept with included task knowledge for enhanced efficiency. It is noteworthy that *Grasping* represents a common task in both industrial and non-industrial settings.

Note that all the described experiments were conducted employing the collaborative lightweight robot Franka Emika Panda and by the authors only.

A. Experimental setup

Two assumptions were used concerning the safe velocity limit v^{SMU} . First, calculating v^{SMU} is based only on available data from the head and chest collisions [2]. In [2], the authors also fitted a curve to the chest collision data and reached the following safety curve that we use too:

$$v^{\text{SMU}} = 0.1 \cdot (-0.4186 m_r + 5.2040), \quad (4)$$

with m_r being the instantaneous robot effective mass, lower cut-off at 0.1 m/s and upper one at 4.5 m/s. Second, as the experiment was performed on a robot already designed to be lightweight and safe, a scaling factor of 0.1 was therefore used for the safety curve to demonstrate the concept; see also [32].⁴

We used the Franka Emika Panda Hand as a gripper, with a minimum contact area of 1 mm². Because the biomechanical data used in SMU are based on various shapes of POIs, the resulting v^{SMU} can be considered safe, especially after the application of the scaling factor.

⁴Detailed motivation for the value of this scaling factor is beyond the scope of this paper, but it is tied to the automotive industry origin of the collision data in the SMU framework [2].

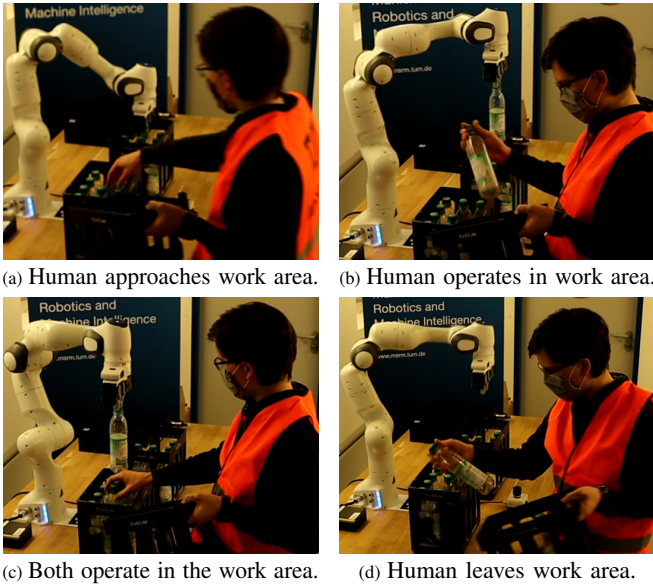


Fig. 5: Experiment progression.

The performance of the shaping approaches is compared in terms of relative productivity (calculated as the time needed to finish the task successfully) against the no-human case, i. e., executing the task with v^{task} .

B. Comparison experiment

This experiment compares pure coexistence and collaboration scenarios. We execute two tasks following the functional modes described in Sec. III to compare the performance of various velocity-shaping approaches under different robot functional modes. The robot end-effector was commanded to execute only a linear Cartesian movement to achieve higher peak velocities and easily interpretable data. Nonetheless, the methodology would also be applicable to more complex robot tasks.

The first task was a pure coexistence scenario between the human partner and the robot, i. e., where both human and robot share the same workspace. However, the robot's behavior is not affected by the human partner's actions. The second task represented a real-time human-robot collaborative scenario with frequent activation of the robot's *Col* mode.

We recorded two interactive human motions (one for each task type, *Data 1* and *Data 2*). For each recording, we ran the human motion cycles five times with given velocity shaping approaches as discussed in Sec. III-B. The goal is to compare their resulting robot performance under the same human actions.

C. Grasping experiment

We consider a collaborative packaging scenario to demonstrate the usage of additional task knowledge to guide safe execution. A bottle is picked up by the robot and moved to a target position while the human partner simultaneously grasps something in the robot's work area, see Fig. 5. As a result, an unintended collision between the human and robot may occur, and appropriate mode switching is being performed. We ran the experiment four times with the prerecorded human tracking data. Similar to the first scenario, the robot used different velocity shaping approaches to complete the task.

Since part of the collaborative task involved vertical downwards robot motion (to grasp a bottle with possible human hand interference), we set the safety performance index as $SP=0$ to enforce the safety-critical behavior for this part of the task. Otherwise, it is set as $SP=1$. Since no human was nearby, this grasping motion was executed with a full task speed of 0.5 m/s.

V. RESULTS AND DISCUSSION

A. Comparison of experimental results

Pure coexistence scenario

A typical robot speed motion profile using human position and velocity information for shaping the robot velocity in a pure coexistence scenario is shown in Fig. 6 (left). In this experiment, the relative speed between robot and human v_{rel} is shaped by changing the robot speed so that the *SMU* is only activated when needed and just as much as needed, respecting the biomechanical safety curve's limit. More specifically, for the shown profiles, the relative human-robot velocity is shaped when needed using the approach v^{short} . The calculated reference acceleration and jerk profiles are also shown together with their smoothed averages. The robot's velocity is continuously changing because the robot is responsive to human motion, and thus, velocity shaping is activated frequently. This makes the robot motion a bit jerky (e. g., at 2 s), but still far below the robot capability thresholds.

Both used approaches for relative velocity shaping during the experiments (i. e., v^{motion} and v^{short}) ensure human safety. When there is a collision risk, the human partner's safety is guaranteed by the relative velocity respecting the used safety curve (Eq. 4). Both approaches result in nearly the same productivity, see Fig. 7 (top, left). However, Fig. 7 (bottom, left) shows that the v^{short} approach results in higher jerk on average. The stronger dependency on the human data for v^{short} is the probable cause of this jerk. Additionally, the approach v^{SMU} has a higher jerk on average than when using v^{task} , since the calculation of the v^{SMU} uses the configuration-dependent robot effective mass [33], so-called reflected mass $m_u(\mathbf{q})$ that changes during the task execution.

The human velocity data was noisy in the given setup. This could be a possible explanation for the lower performance of highly sensitive velocity shaping (v^{motion} and v^{short}) as opposed to the performance of the approach using only the distance information, i. e., approach v^{SMU} .

Collaborative scenario

A typical robot speed motion profile for the involved collaborative task, together with the recorded human interaction, is shown in Fig. 6 (right). The corresponding productivity and average jerk levels are also depicted in Fig. 7 (right). Relying on a very primitive *SMU* implementation in which only the human distance is used to trigger robot velocity shaping gives relatively shorter task execution times. As a result, the productivity is not that much sacrificed with around 80% when compared to using v^{task} . However, this approach is oversimplistic and does not take into account the human speed v_H , which leads to unsafe situations if v_H is increasing in the robot motion direction \mathbf{u} as the resulting collision velocity would exceed the safe relative velocity.

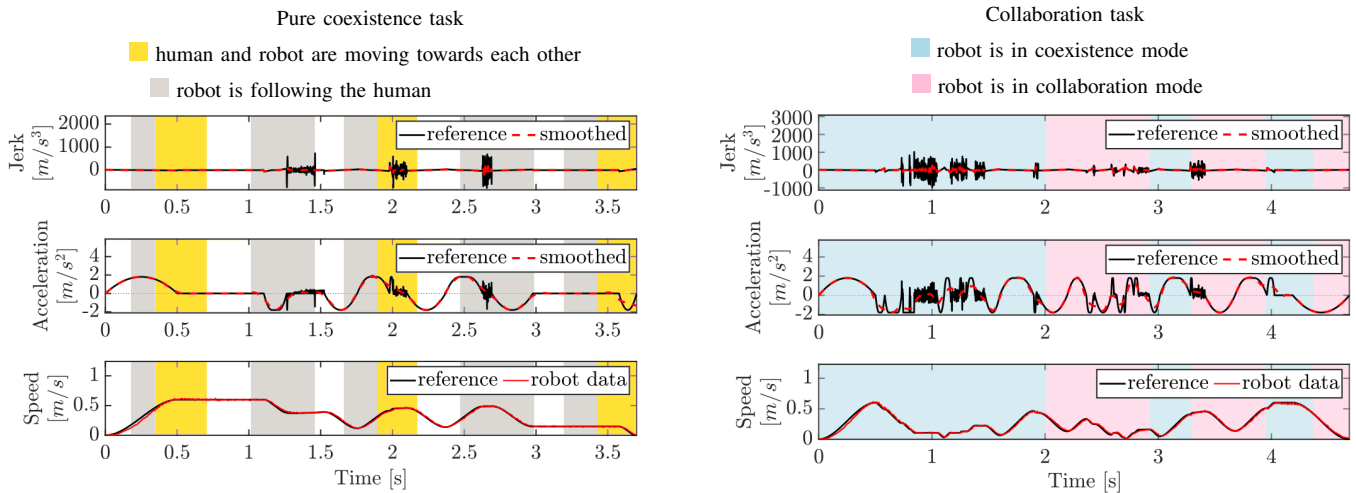


Fig. 6: Safe task execution under two human-robot interactive scenarios: pure coexistence (left) and collaboration (right). The figures contain smoothed evolution of the noisy reference data (*smoothed*) and the actual measured *robot data* as opposed to the commanded *reference*.

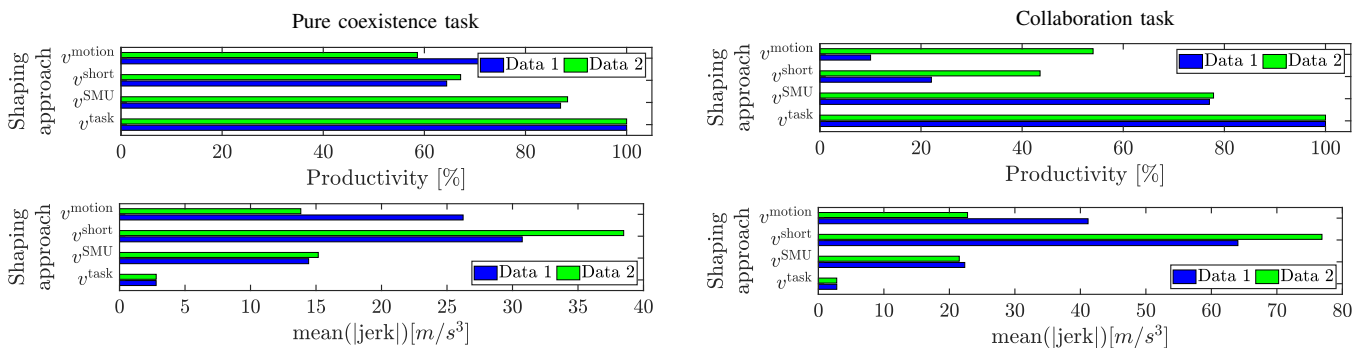


Fig. 7: Task productivity (top) and average jerk levels (bottom) of different approaches for safe velocity shaping in the coexistence (left) and collaboration (right) scenarios as compared against the case when no human is around (i.e., the robot mode is in the autonomous mode).

Using the approach v^{motion} gives the worst performance in terms of productivity as compared to approach v^{short} . Overall, higher productivity is achieved at the cost of higher jerk levels that are caused by continuous velocity shaping.

B. Grasping experiment results

A robot speed motion profile for the involved collaborative task while using velocity shaping along its motion direction, i.e., v^{motion} , is shown in Fig. 8 (bottom row).

The following task execution times were obtained when comparing different velocity-shaping approaches for the same prerecorded human motion. The reference execution time when using full task speed v^{task} was 6.17 s. Using only the relative human-robot distance information for safe velocity shaping (i.e., approach v^{SMU}) the task execution takes 7.20 s, whereas using approach v^{short} it takes 7.34 s. Finally, with the depicted v^{motion} shaping approach 7.30 s is needed to finish the grasping task safely.

VI. CONCLUSION

This work presented a transfer of experiences concerning safety of physical human-robot interaction from industrial settings to non-industrial robots, in addition to a method for an efficient combination of interaction modes and safety. This integration used the *Safe Motion Unit* scheme with human keypoint detection and a smooth velocity shaping controller. The proposed approach is evaluated with various relative velocity measures and expected interaction modes. However,

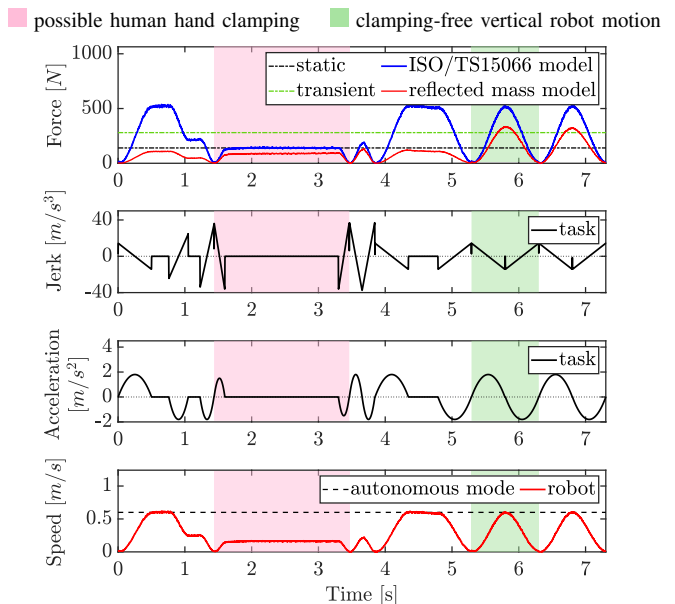


Fig. 8: Robot motion profile for the Grasping experiment with the inclusion of task knowledge of possible human hand clamping. A similar vertical robot motion without human interference is also shown for comparison. The figure shows the force limits given by the standard for the quasi-static or transient collisions. We differentiate cases where the human hand interference is excluded (shaded green area) or expected (shaded red area).

it was found that higher task performance comes at the price of higher jerk levels for the robot velocity shaping while moving.

While industrial safety standards are not binding for non-

industrial robots, the highly developed research on safe physical human-robot interaction for industrial applications also provides a sound inspiration for non-industrial interactions. Future research should focus on the specifics of various non-industrial interaction scenarios as they represent new challenges from the industrial context. For example, service robots are connected with close physical interaction, leading to many occlusions of the vision system or the demand for physical contact. These might necessitate using sensors other than an RGB-D camera (e.g., artificial sensitive skin). Therefore, this integration of additional sensors and their synthesis should be investigated next. Another direction should be to consider the human behavior with respect to the robot motion as in the case of the Expectable Motion Unit [28].

ACKNOWLEDGMENT

P.S. and M.H. were supported by the Ministry of Industry and Trade of the Czech Republic (OPPIK, project no. CZ.01.1.02/0.0/0.0/19_264/0019867). M.H. was additionally supported by the OP VVV MEYS funded project “Research Center for Informatics” (no. CZ.02.1.01/0.0/0.0/16_019/0000765). The authors from TU Munich acknowledge the support of: the European Union’s Horizon 2020 research and innovation program as part of the projects I.AM. (grant no. 871899) and DARKO (grant no. 101017274). They also thank the Bavarian State Ministry for Economic Affairs, Regional Development, and Energy (StMWi) for financial support as part of the project SafeRoBAY (grant no. DIK0203/01).

Please note that S. Haddadin has a potential conflict of interest as a shareholder of Franka Emika GmbH.

REFERENCES

- [1] International Organization for Standardization (ISO), “Robots and robotic devices - Collaborative robots (ISO/TS 15066:2016),” 2016.
- [2] N. Mansfeld, M. Hamad, M. Becker, A. G. Marin, and S. Haddadin, “Safety Map: A Unified Representation for Biomechanics Impact Data and Robot Instantaneous Dynamic Properties,” *IEEE Robotics and Automation Letters (RA-L)*, vol. 3, no. 3, pp. 1880–1887, Jul. 2018.
- [3] D. Han, M. Y. Park, H. Shin, K. S. Kim, and S. Rhim, “Identifying Safety Conditions of Human-Robot Collision based on Skin Injury Analysis,” in *2018 15th International Conference on Ubiquitous Robots (UR)*. IEEE, 2018, pp. 420–423.
- [4] E. Fosch Villaronga, “ISO 13482: 2014 and its confusing categories. Building a bridge between law and robotics,” in *New trends in medical and service robots*. Springer, 2016, pp. 31–44.
- [5] T. Jacobs and G. S. Virk, “ISO 13482-The new safety standard for personal care robots,” in *ISR/Robotik 2014; 41st International Symposium on Robotics*. VDE, 2014, pp. 1–6.
- [6] International Organization for Standardization (ISO), “Robots and Robotics Devices - Safety Requirements for Personal Care Robots,” 2014.
- [7] M. Tröbinger, C. Jähne, Z. Qu, J. Elsner, A. Reindl, S. Getz, T. Goll, B. Loinger, T. Loibl, C. Kugler *et al.*, “Introducing GARMi-a service robotics platform to support the elderly at home: design philosophy, system overview and first results,” *IEEE Robotics and Automation Letters*, vol. 6, no. 3, pp. 5857–5864, 2021.
- [8] MIRMI - Robotics and Machine Intelligence, “GARMi Concept - Robot Assistant for the Elderly,” 2019. [Online]. Available: <https://www.youtube.com/watch?v=vqq7S31FGFc>
- [9] Z. Cao, G. Hidalgo Martinez, T. Simon, S. Wei, and Y. A. Sheikh, “OpenPose: Realtime Multi-Person 2D Pose Estimation using Part Affinity Fields,” *IEEE Transactions on Pattern Analysis and Machine Intelligence*, 2019.
- [10] F. Vicentini, “Terminology in safety of collaborative robotics,” *Robotics and Computer-Integrated Manufacturing*, vol. 63, p. 101921, 2020.
- [11] D. Henrich and S. Kuhn, “Modeling intuitive behavior for safe human/robot coexistence cooperation,” in *Proceedings 2006 IEEE International Conference on Robotics and Automation, 2006. ICRA 2006*. IEEE, 2006, pp. 3929–3934.
- [12] F. Flacco and A. De Luca, “Safe physical human-robot collaboration,” in *2013 IEEE/RSJ International Conference on Intelligent Robots and Systems*. IEEE, 2013, pp. 2072–2072.
- [13] S. Haddadin, M. Suppa, S. Fuchs, T. Bodenmüller, A. Albu-Schäffer, and G. Hirzinger, “Towards the robotic co-worker,” in *Robotics Research*. Springer, 2011, pp. 261–282.
- [14] S. Haddadin and E. Croft, “Physical Human-Robot Interaction,” in *Handbook of Robotics*, 2nd ed., B. Siciliano and O. Khatib, Eds. Springer, 2016.
- [15] P. A. Lasota, T. Fong, J. A. Shah *et al.*, *A survey of methods for safe human-robot interaction*. Now Publishers Delft, The Netherlands, 2017, vol. 104.
- [16] F. Vicentini, “Collaborative robotics: a survey,” *Journal of Mechanical Design*, vol. 143, no. 4, 2021.
- [17] F. Fabrizio and A. De Luca, “Real-time computation of distance to dynamic obstacles with multiple depth sensors,” *IEEE Robotics and Automation Letters*, vol. 2, no. 1, pp. 56–63, 2016.
- [18] A. K. Pandey and R. Gelin, “A mass-produced sociable humanoid robot: Pepper: The first machine of its kind,” *IEEE Robotics & Automation Magazine*, vol. 25, no. 3, pp. 40–48, 2018.
- [19] M. Miyagawa, Y. Kai, Y. Yasuhara, H. Ito, F. Betriana, T. Tanioka, R. Locsin *et al.*, “Consideration of safety management when using pepper, a humanoid robot for care of older adults,” *Intelligent Control and Automation*, vol. 11, no. 01, p. 15, 2019.
- [20] R. Weitschat and H. Aschemann, “Safe and efficient human-robot collaboration Part II: Optimal generalized human-in-the-loop real-time motion generation,” *IEEE Robotics and Automation Letters (RA-L)*, vol. 3, no. 4, pp. 3781–3788, 2018.
- [21] A. Palleschi, M. Hamad, S. Abdolshah, M. Garabini, S. Haddadin, and L. Pallottino, “Fast and safe trajectory planning: Solving the cobot performance/safety trade-off in human-robot shared environments,” *IEEE Robotics and Automation Letters*, vol. 6, no. 3, pp. 5445–5452, 2021.
- [22] A. M. Zanchettin, N. M. Ceriani, P. Rocco, H. Ding, and B. Matthias, “Safety in human-robot collaborative manufacturing environments: Metrics and control,” *IEEE Transactions on Automation Science and Engineering*, vol. 13, no. 2, pp. 882–893, 2016.
- [23] A. M. Zanchettin, A. Casalino, L. Piroddi, and P. Rocco, “Prediction of human activity patterns for human-robot collaborative assembly tasks,” *IEEE Transactions on Industrial Informatics*, vol. 15, no. 7, pp. 3934–3942, 2018.
- [24] A. M. Zanchettin, P. Rocco, S. Chiappa, and R. Rossi, “Towards an optimal avoidance strategy for collaborative robots,” *Robotics and Computer-Integrated Manufacturing*, vol. 59, pp. 47–55, 2019.
- [25] N. Lucci, B. Lacevic, A. M. Zanchettin, and P. Rocco, “Combining speed and separation monitoring with power and force limiting for safe collaborative robotics applications,” *IEEE Robotics and Automation Letters*, vol. 5, no. 4, pp. 6121–6128, 2020.
- [26] M. Huber, M. Rickert, A. Knoll, T. Brandt, and S. Glasauer, “Human-robot interaction in handing-over tasks,” in *RO-MAN 2008-The 17th IEEE International Symposium on Robot and Human Interactive Communication*. IEEE, 2008, pp. 107–112.
- [27] R. J. Kirschner, L. Burr, M. Porzenheim, H. Mayer, S. Abdolshah, and S. Haddadin, “Involuntary motion in human-robot interaction: Effect of interactive user training on the occurrence of human startle-surprise motion,” in *2021 IEEE International Conference on Intelligence and Safety for Robotics (ISR)*. IEEE, 2021, pp. 28–32.
- [28] R. J. Kirschner, H. Mayer, L. Burr, N. Mansfeld, S. Abdolshah, and S. Haddadin, “Expectable Motion Unit: Avoiding Hazards From Human Involuntary Motions in Human-Robot Interaction,” *IEEE Robotics and Automation Letters*, 2022.
- [29] P. Svarny, M. Tesar, J. K. Behrens, and M. Hoffmann, “Safe physical HRI: Toward a unified treatment of speed and separation monitoring together with power and force limiting,” in *2019 IEEE/RSJ International Conference on Intelligent Robots and Systems (IROS)*, 2019, pp. 7580–7587.
- [30] G. Bradski, “The OpenCV Library,” *Dr. Dobb’s Journal of Software Tools*, 2000.
- [31] L. Biagiotti and C. Melchiorri, *Trajectory Planning for Automatic Machines and Robots*. Springer-Verlag Berlin Heidelberg, 2008.
- [32] S. Haddadin, S. Haddadin, A. Khoury, T. Rokahr, S. Parusel, R. Burgkart, A. Bicchi, and A. Albu-Schäffer, “On making robots understand safety: Embedding injury knowledge into control,” *The International Journal of Robotics Research (IJRR)*, vol. 31, no. 13, pp. 1578–1602, 2012.
- [33] O. Khatib, “Inertial properties in robotic manipulation: An object-level framework,” *The International Journal of Robotics Research*, vol. 14, no. 1, pp. 19–36, 1995.